Surgery 164 (2018) 165–172

Contents lists available at ScienceDirect

Surgery

journal homepage: www.elsevier.com/locate/surg

Pediatrics

Synthetic high-density lipoprotein nanoconjugate targets neuroblastoma stem cells, blocking migration and self-renewal☆

Chitra Subramanian, PhD, MBA[a], Peter T. White, MD[a], Rui Kuai, PhD[b,c], Avinaash Kalidindi, BS[a], Valerie P. Castle, MD[d], James J. Moon, PhD[b,c], Barbara N. Timmermann, PhD[e], Anna Schwendeman, PhD[b,c], Mark S. Cohen, MD, FACS[a,f,*]

[a] Department of Surgery, University of Michigan, Ann Arbor, MI
[b] Department of Pharmaceutical Sciences, University of Michigan, Ann Arbor, MI
[c] Biointerfaces Institute, University of Michigan, Ann Arbor, MI
[d] Department of Pediatrics, University of Michigan, Ann Arbor, MI
[e] Department of Medicinal Chemistry, University of Kansas, Lawrence, KS
[f] Department of Pharmacology, University of Michigan, Ann Arbor, MI

ARTICLE INFO

Article history:
Accepted 13 January 2018
Available online 10 May 2018

ABSTRACT

Background: Pathways critical for neuroblastoma cancer stem cell function are targeted by 4,19,27-triacetyl withalongolide A (WGA-TA). Because neuroblastoma cells and their cancer stem cells highly overexpress the scavenger receptor class B type 1 receptor that binds to synthetic high-density lipoprotein, we hypothesized that a novel mimetic synthetic high-density lipoprotein nanoparticle would be an ideal carrier for the delivery of 4,19,27-triacetyl withalongolide to neuroblastoma and neuroblastoma cancer stem cells.

Methods: Expression of scavenger receptor class B type 1 in validated human neuroblastoma cells was evaluated by quantitative polymerase chain reaction (qPCR) and Western blot. In vitro cellular uptake of synthetic high-density lipoprotein nanoparticles was observed with a fluorescence microscope. In vivo biodistribution of synthetic high-density lipoprotein nanoparticles was investigated with IVIS imaging. Self-renewal and migration/invasion were assessed by sphere formation and Boyden chamber assays, respectively. Viability was analyzed by CellTiter-Glo assay. Cancer stem cell markers were evaluated by flow cytometry.

Results: qPCR and Western blot analysis revealed a higher level of scavenger receptor class B type 1 expression and drug uptake in N-myc amplified neuroblastoma cells. In vitro uptake of synthetic high-density lipoprotein was almost completely blocked by excess synthetic high-density lipoprotein. The synthetic high-density lipoprotein nanoparticles mainly accumulated in the tumor and liver, but not in other organs. Synthetic HDL-4,19,27-triacetyl withalongolide showed a 1,000-fold higher potency than the carrier (synthetic high-density lipoprotein) alone ($P < .01$) to kill neuroblastoma cells. Additionally, a dose-dependent decrease in sphere formation, invasion, migration, and cancer stem cell markers was observed after treatment of neuroblastoma cells with synthetic high-density lipoprotein–4,19,27-triacetyl withalongolide A.

Conclusion: Synthetic high-density lipoprotein is a promising platform to improve the delivery of anticancer drug 4,19,27-triacetyl withalongolide A to neuroblastomas and neuroblastoma cancer stem cells through SR-B1 targeting in vitro and in vivo.

Neuroblastoma (NB) accounts for approximately 15% of cancer-related pediatric deaths and is the most common extracranial solid tumor affecting children.[1] Despite aggressive combination therapy options, over 50% of children with high-risk disease will relapse within the first 5 years after diagnosis.[2,3] In patients whose disease progresses or relapses, median survival drops to less than 1 year, and the 10-year overall survival (OS) is abysmal (6.8% for patients who progress and 14.4% for patients who relapse).[4] In addition to a poor OS, surviving patients with high-risk NBs are often left with

☆ Supported by the National Institutes of Health (T32 CA009672, R01 CA173292), NIH 3U01-CA-120458-03, the University of Michigan Comprehensive Cancer Center Support Grant P30-CA-046592, and the University of Michigan Department of Surgery. Presented at the 11th Annual Academic Surgical Congress in Jacksonville, FL, February 2–4, 2016.

* Corresponding author. Department of Surgery, 2920K Taubman Center SPC 5331, University of Michigan Hospital and Health Systems, 1500 E. Medical Center Dr., Ann Arbor, MI 48109-5331.

E-mail addresses: cohenmar@med.umich.edu, cohenmar@umich.edu (M.S. Cohen).

https://doi.org/10.1016/j.surg.2018.01.023
0039-6060/

considerable long-term deficits, including hearing loss, cardiac dysfunction, infertility, secondary malignancies, learning disabilities, and vision and skeletal problems, along with many others. Collectively, this underscores the critical and urgent need for the development of more effective and less toxic therapies for treating NB.[5]

Currently, targeted therapies using antiangiogenic drugs, anaplastic lymphoma kinase antagonists, and PI3K/Akt/mTOR inhibitors are in phase I/II clinical trials either alone or in combination with conventional chemotherapy for refractory or recurrent NB.[6] A major limitation to which each of these treatments is susceptible is that cancer cells have an innate ability to develop resistance to single-target drugs through several mechanisms, including recruitment or up-regulation of alternative survival pathways. It has been postulated that this drug resistance may in part be due to the presence of a small population of progenitor cells called cancer stem cells (CSCs) that can escape resistance and recapitulate the tumor and form spheres. For the last 6 years, our group has been studying the multitargeted anticancer benefits of natural withanolides isolated from the *Physalis* plant.[7–14] Not only are these natural products extremely safe in vivo with a large therapeutic index, but they also function through a unique mechanism of action, leading to the simultaneous and selective inhibition of multiple key regulatory pathways in cancers. In NB cells, withanolides target the specific pathways involved in their rapid proliferation, invasion, metastatic spread, poor survival, and escape resistance. These natural compounds utilize a multitargeted approach through their unique mechanism of action, inducing an oxidative stress response coupled with a novel means of inhibiting heat shock protein (HSP90) chaperone function through blockade of CDC37 docking, thereby preventing kinase activation by HSP90.[10] In NBs, these mechanisms target key tumorigenic proteins that are implicated in NB-CSC functions, such as invasion, drug resistance, and poor survival.[8,15–17] Because withanolides are safe and selective and carry potent multitargeted anticancer effects in NB, they represent a novel yet suitable drug strategy to overcome many of the barriers identified for the successful treatment of NBs.

Despite being effective anticancer therapeutics both in vitro and in vivo, withanolides have low solubility in plasma and a short circulation half-life of only 1 hour,[18] limiting their translational and clinical suitability. To overcome these limitations, we have developed the unique approach of encapsulating withanolides in synthetic high-density lipoprotein (sHDL) nanoparticles. These nanoparticles offer several advantages over other synthetic nanocarriers, including liposomes, micelles, and inorganic and polymeric nanoparticles. Most notably, they have an ultrasmall size (8–12 nM in diameter), are already in numerous clinical trials with excellent safety and tolerability in humans, and have a long circulating half-life.[11] In addition to improved circulation and stability, the sHDL nanoparticles target tumor cells via their highly overexpressed surface receptor, scavenger receptor class B type 1 (SR-B1), for which HDL is a ligand.[19] Hence, in the present study we have developed a novel synthetic HDL mimetic nanoparticle (sHDL) to encapsulate 4,19,27-triacetyl withalongolide A (WGA-TA) and evaluated particle and drug uptake as well as the efficacy of SR-B1-mediated targeting of NB cancer stem cell functions such as migration, invasion, and sphere formation.

Methods

Cell lines

Human NB cell lines SH-EP, SH-SY5Y, IMR-32, and SK-N-AS were validated as authentic by standard DNA fingerprinting and were grown in 2D culture. The cells were grown in Minimum Essential Medium (MEM) (Thermo Fisher, Rockville, MD) supplemented with 10% fetal bovine serum (FBS) (Sigma Chemical Co, St. Louis, MO) and 1% penicillin and streptomycin (Thermo Fisher). For the growth of IMR-32 cells, the media was additionally supplemented with 1% MEM Non-Essential Amino Acids (100X; Sigma Chemical Co), 2 mmol/L of L-Glutamine (200 mmol/L; Sigma Chemical Co), 1 mmol/L sodium pyruvate (100 mm/L; Sigma Chemical Co), and 1,500 mg/L of sodium bicarbonate (7.5%; Sigma Chemical Co). The cell lines were incubated at 37 °C in a humidified atmosphere of 5% CO_2 in air.

Preparation of sHDL WGA-TA nanoparticles

sHDL nanoparticles were loaded with either the dye [DiO (benzoxazolium, 3-octadecyl-2-[3-(3-octadecyl-2(3H)-benzoxazolyliden e)-1-propenyl]-, perchlorate), or DiR (DilC$_{18}$(7) (1,1′-dioctadecyl-3,3,3′,3′-tetramethylindotricarbocyanine iodide)] or the drug withanolide (WGA-TA), using the lyophilization method as described in our previous reports.[20]

Cell proliferation assay

Approximately 5,000 NB cells per well were seeded in a 96-well plate in triplicate. As a control, WGA-TA alone, sHDL alone, and untreated cells were used. Following 24 hours' incubation time, cells were treated with serial dilutions of either sHDL or sHDL-WGA-TA or WGA-TA starting at 20 μM. Viability after 72 hours was evaluated by CellTiter-Glo luminescent assay as per the manufacturer's protocol (Promega Corp, Madison, WI). The luminescence was quantified via a BioTek Synergy Neo plate reader (Bio-Tek, Winooski, VT). Cell viability ratios were calculated using GraphPad Prism 5 software (GraphPad Software, Inc, La Jolla, CA).

Real-time polymerase chain reaction and Western blot analysis for SR-B1

RNA from NB cell lines SK-N-BE(2), IMR-32, SH-EP, SH-SY5Y, SK-N-AS, the positive control NCI-H295R, and the negative control (Jurkat and fibroblast cells) were extracted using Qiagen RNA isolation kit (Qiagen Sciences, Valencia, CA). The 500 ng of RNA was reverse transcribed using superscript RT kit from Thermo Fisher. Quantitative polymerase chain reaction (PCR) was performed in a step-1 real-time PCR machine using SR-B1 and actin specific primer sets. Relative gene expression levels were calculated after normalization with internal controls. The expression of SR-B1 was further confirmed at the protein level by Western blot (WB) analysis as previously described, and actin was used as a loading control.[12]

Uptake of DiO-labeled sHDL nanoparticles by NB cells in vitro

SR-B1-mediated uptake of dye by the NB cell lines as well as the positive control NCI-H295R and the negative control Jurkat was evaluated after incubating the cells for 4 hours with the long-chain dialkylcarbocyanines lipophilic tracer DiO (Invitrogen, Carlsbad, CA) labeled sHDL nanoparticle. Additionally, SR-B1-mediated uptake was further confirmed after small interfering (si)RNA-mediated SR-B1 knockdown by standard protocols. Briefly, SK-N-BE(2) cells grown to 80% confluency were transfected with validated silencer select non-targeting as well as SR-B1 targeting siRNA using Lipofectamine RNAiMAX transfection reagent as per the manufacturer protocol (Thermo Fisher Scientific, Carlsbad, CA). After 48 hours, cells were treated with DiO-labeled sHDL, and part of the cells were collected for WB analysis to verify knockdown of SR-B1. For blocking, the cells were treated with 10-fold excess of blank sHDL for 1 hour prior to the addition of the nanoparticles. The fluorescent images were taken using a Nikon fluorescent microscope after fixing the cells with paraformaldehyde. The nuclei

were stained with 4′, 6-diamidino-2-phenylindole (DAPI), a fluorescent stain binding to DNA.

Sphere formation assay

NB cell lines IMR-32, SK-N-BE(2), and SK-N-AS were plated at a density of approximately 250 cells per well in a 96-well ultralow attachment plate (Corning, Inc, Corning, NY) in mammocult medium (STEMCELL Technologies, Vancouver, BC, Canada) with varying concentrations of sHDL, WGA-TA, and sHDL-WGA-TA starting at 7.7 nM, and the ability of cells to form spheres was observed for 1 week. The number of spheres formed (>25 cells) was counted using a light microscope.

Boyden chamber assay for migration and invasion

NB cell lines IMR-32, SK-N-BE(2), and SK-N-AS cells were suspended in serum-free MEM supplemented with penicillin/streptomycin and 0.5 or 1 μM of medication (WGA-TA, sHDL-WGA-TA, or sHDL). An equal number of cells with the tested drugs were placed on the upper well of either Matrigel-coated 8-μm polycarbonate membranes (Corning, Inc, Corning, NY) or standard membranes, and 10% FBS at the lower well served as a chemoattractant. After 48 hours' incubation, membranes were fixed in 2% paraformaldehyde and stained with 1% crystal violet in 20% methanol for 20 minutes. The membranes were washed with distilled water; nonmigratory cells from the insert interior were removed using cotton-tipped swab. The migration and invasion were quantified as the number of cells per field using a light microscope.

Evaluation of markers of NB CSCs by flow cytometry

IMR-32 and SK-N-BE(2) cells were treated with 0.5μM drugs (WGA-TA, sHDL-WGA-TA, or sHDL) for 24 hours. The cells were collected, washed with phosphate-buffered saline containing 0.5% bovine serum albumin, and then incubated with phycoerythrin-conjugated CD133 or CD114 (Miltenyi Biotec, Bergisch Gladbach, Germany) antibodies for 30 minutes. Following incubation, the cells were washed with phosphate-buffered saline containing 0.5% bovine serum albumin and analyzed by CyAn ADP analyzer (Beckman Coulter, Inc, Fullerton, CA). DAPI staining at 1μg/mL was used to exclude dead cells from analysis.

In vivo distribution of DiR sHDL nanoparticle by IMR-32 xenograft

To characterize the distribution of the nanoparticle, whole-body imaging was conducted on IMR-32 tumor-bearing mice using IVIS imaging at the University of Michigan imaging core. DiR-dye labeled sHDL (0.6% DiR) was injected intraperitoneally at 1 mg/kg dose, and the whole-body imaging was performed after 24 hours. At the end of 24 hours, animals were killed and major organs including the spleen, liver, heart, lung, kidneys, and tumor were harvested, weighed, and imaged to characterize the biodistribution of DiR-sHDL.

Statistical analysis

All the experiments were repeated in triplicate, and the values are presented as average ± standard deviation. The *P* values were calculated by 1-way analysis of variance using Dunnett's multiple comparison test using GraphPad Prism 5 software (GraphPad Software, Inc, La Jolla, CA).

Results

HDL receptor SR-B1 is highly expressed in N-myc amplified NB cells

For sHDL-WGA-TA to specifically target malignant NB cells, high levels of the HDL receptor SR-B1 expression are necessary. Therefore, we examined both messenger RNA (mRNA) and protein levels of SR-B1 in NB cells as well as in SR-B1 negative and positive control cell lines by real-time PCR (Fig 1, *A*) and WB analysis (Fig 1, *B*). Compared to the negative control (fibroblast and Jurkat) cell lines, mRNA level expression of SR-B1 for N-myc amplified (IMR-32 and SK-N-BE[2]) and nonamplified (SH-EP, SK-N-AS, and SH-SY5Y) cell lines were 6- to 7-fold and 1- to 3-fold higher, respectively ($P < .001$ vs controls). Results were similar for the protein expressions of SR-B1 as N-myc amplified cells expressed 18-fold higher levels of SR-B1 compared to negative control cells ($P < .001$), whereas nonamplified cells expressed only 6- to 8-fold higher levels of SR-B1 protein compared to the negative controls ($P < .05$). As expected, the positive control adrenocortical carcinoma cell line, NCI-H295R, had very high mRNA and protein expression levels of SR-B1 versus the negative control or the NB cell lines ($P < .0001$).

NB cells uptake DiO sHDL nanoparticles in vitro through its receptor SR-B1

The ability of NB cancer cells with various levels of SR-B1 to take up the sHDL nanoparticles through SR-B1 receptor and the effect of sHDL composition on internalization of sHDL's cargo by SR-B1 was examined after a 4-hour incubation of cells with DiO-labeled sHDL. The cellular uptake of the nanoparticle showed increased uptake for SR-B1 high expressers (IMR-32, SK-N-BE[2], and the positive control) compared to the low expressers (SH-EP and SK-N-AS) and the negative control. To further confirm that the uptake was mediated through SR-B1, the cells were either pretreated with 10-fold excess of sHDL or SR-B1 was knocked down using siRNA and then DiO-labeled nanoparticles were added. As expected, the uptake was completely blocked by either excess sHDL or by knocking down SR-B1 (Fig 2, *A* and *B*), indicating receptor-mediated uptake of the drug by NB cells.

WGA-TA encapsulated sHDL nanoparticle reduces the viability of NB cells

The viability of sHDL nanoparticles either alone or after encapsulation with WGA-TA was determined by CellTiter-Glo assay (Fig 3). Treatment of cells with sHDL nanoparticle alone had minimal effect on the viability of cells (IC_{50} >10μM), whereas treatment with either WGA-TA or sHDL-WGA-TA was highly effective in reducing the viability of NB cells at nM concentrations ($IC_{50} = 25–55$ nM), which was 4- to 10-fold greater than that of normal fibroblast cells (Table).

WGA-TA encapsulated sHDL nanoparticle targets NB CSCs

To evaluate whether the novel WGA-TA encapsulated sHDL nanoparticle targets NB cancer stem cells, sphere formation assay (indicator of stem like cells) and analysis of CSC markers (CD114 and CD133), Boyden chamber migration, and invasion assays were performed. Starting at a very low concentration of 7.8 nM, the drugs prevented sphere formation in a dose-dependent manner, and at about 62.5-125 nM sphere formation was completely prevented compared to either the control or sHDL nanoparticle treated cells ($P < .001$). This indicated that sHDL-WGA-TA particles likely target NB CSCs (Fig 4). Analysis of markers of CSCs revealed 40% to 50% and 10% to 20% decreases in the levels of markers CD133 and CD114, respectively, after treatment with either

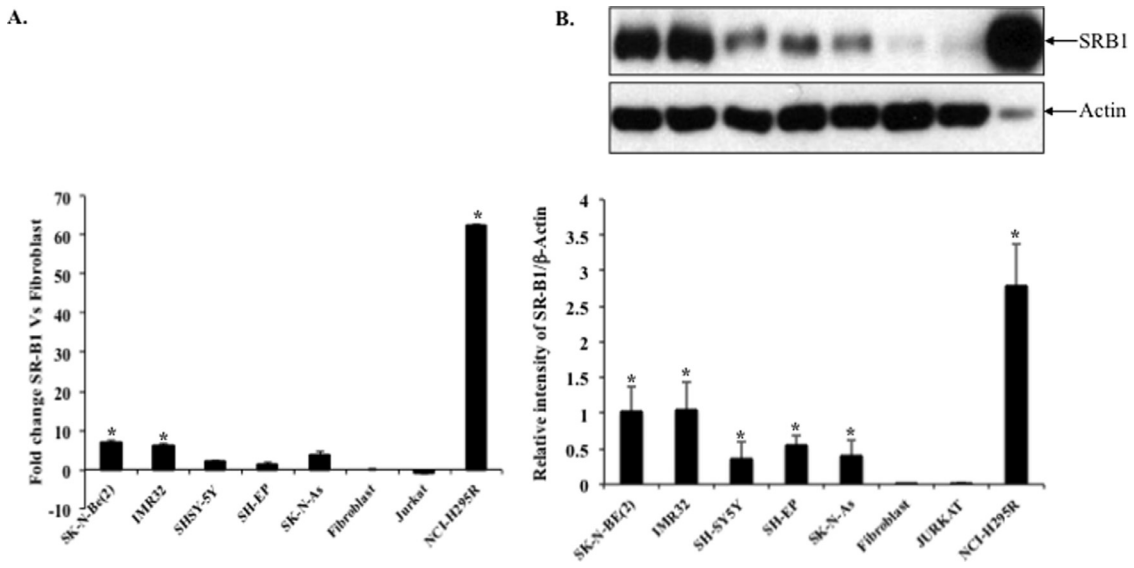

Fig. 1. (*A* and *B*) Expression levels of SR-B1 in NB cell lines. mRNA and protein levels of SR-B1 in both N-myc amplified and non-amplified cell lines by real-time PCR and WB analysis. As a positive control, NCI-H295R was used. Jurkat and fibroblast cell lines were used as negative control. mRNA level expression was measured by standard curve method using actin as an internal control. As a loading control for WB, the same blot was stripped and probed for actin.

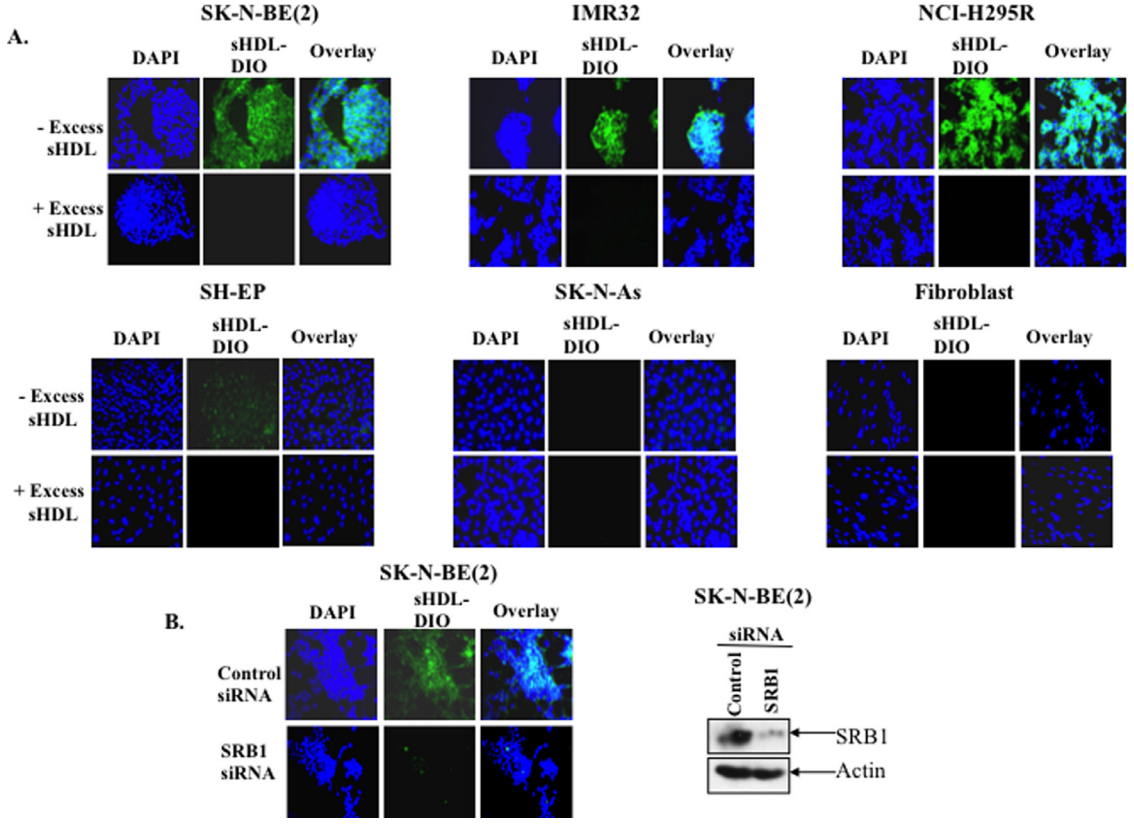

Fig. 2. (*A* and *B*) In vitro uptake of DiO-labeled sHDL nanoparticle by NB cells. SR-B1 high- and low-expressing NB cells, positive control (NCI-H295R), and negative control (Jurkat and fibroblast) cell lines were treated with DiO-labeled sHDL nanoparticle (green) for 4 hours, and the accumulation of the nanoparticle was examined using a fluorescent microscope. The nuclei of the cells were labeled with DAPI (blue). The cells were either pretreated with sHDL for 1 hour or SR-B1 was knocked down to block the HDL receptor and uptake was imaged using a fluorescent microscope. The knockdown efficiency was verified by WB analysis.

WGA-TA or sHDL-WGA-TA compared to controls ($P < .01$), whereas sHDL alone showed no significant changes in levels compared to control for both IMR-32 and SK-N-BE(2) cells (Fig 5). Another important property of cancer cells is migration leading to metastasis. Therefore, we analyzed migration and invasion of NB cells through Boyden chamber (Fig 6). Treatment of NB cells with 1 μM sHDL-WGA-TA or WGA-TA for 48 hours was highly effective in blocking the migration and invasion of cells, whereas sHDL alone did not have any effect.

IMR-32 xenografts uptake DiR sHDL nanoparticle in vivo

To assess the biodistribution of the sHDL nanoparticles, whole-animal imaging and ex vivo imaging of major organs of

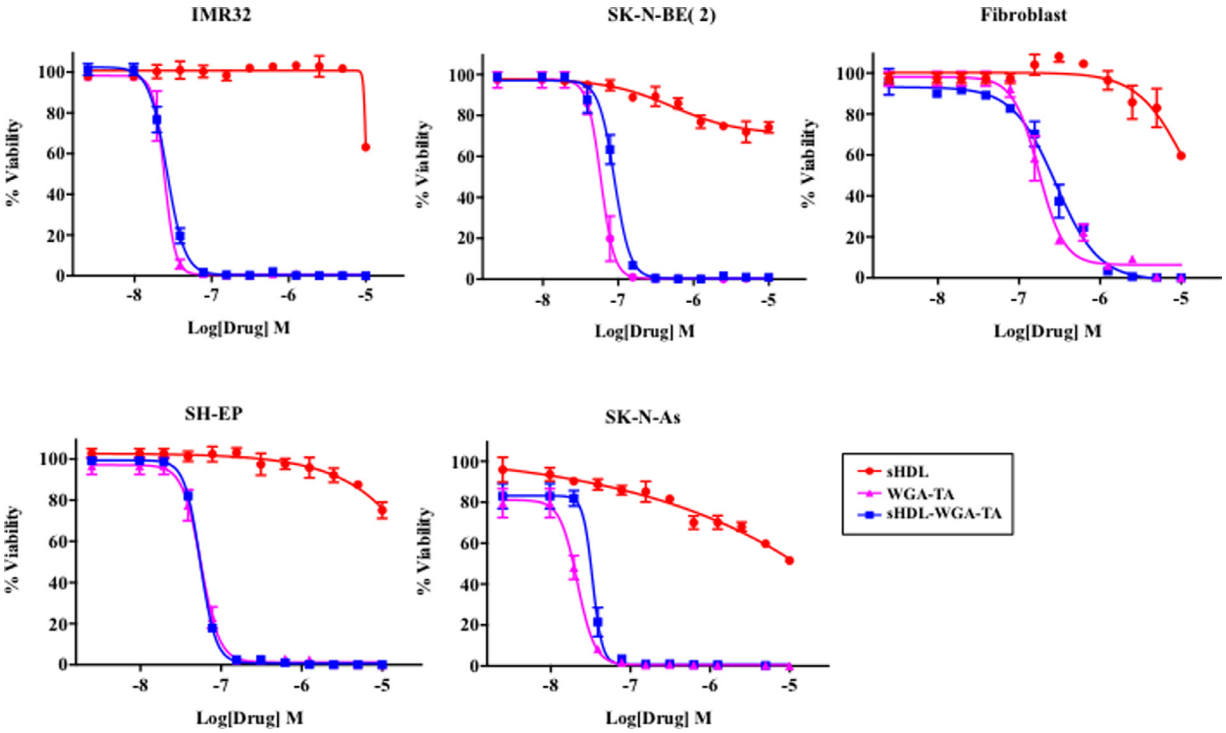

Fig. 3. In vitro viability of NB cells after drug treatment. The viability of NB cells, NCI-H295R, and fibroblasts were determined after treating the cells with varying concentrations of either sHDL or WGA-TA or sHDL-WGA-TA nanoparticle. Percentage viability was determined by MTS assay, and the IC50 values were calculated using GraphPad Prism software (see the Table).

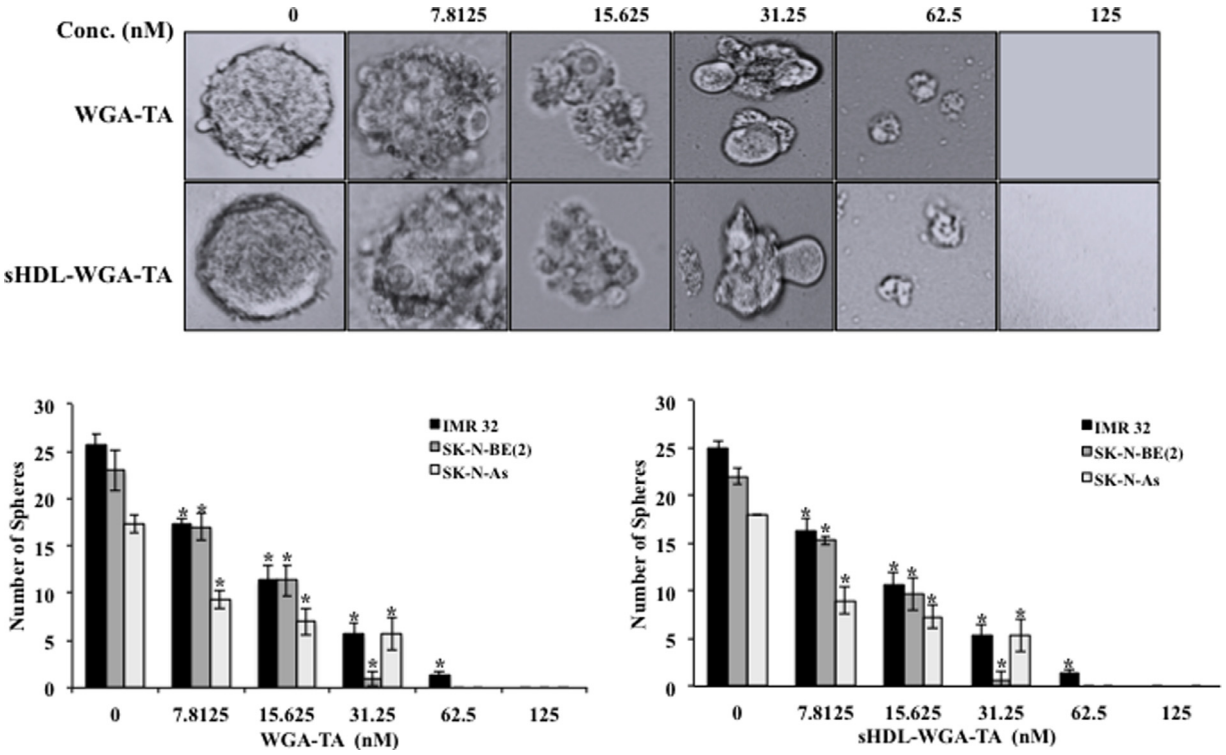

Fig. 4. Concentration-dependent prevention of self-renewal of NB cells by WGA-TA–loaded sHDL and WGA-TA. Sphere formation after treatment of NB cells (IMR-32, SK-N-BE(2), and SK-N-AS) with varying concentrations of either sHDL or WGA-TA or sHDL-WGA-TA nanoparticles for a week was examined by counting the number of spheres (>50 cells per sphere) formed under a light microscope. All experiments were repeated thrice, and the values are represented as mean ± standard deviation. Representative spheres from IMR-32 cells are shown.

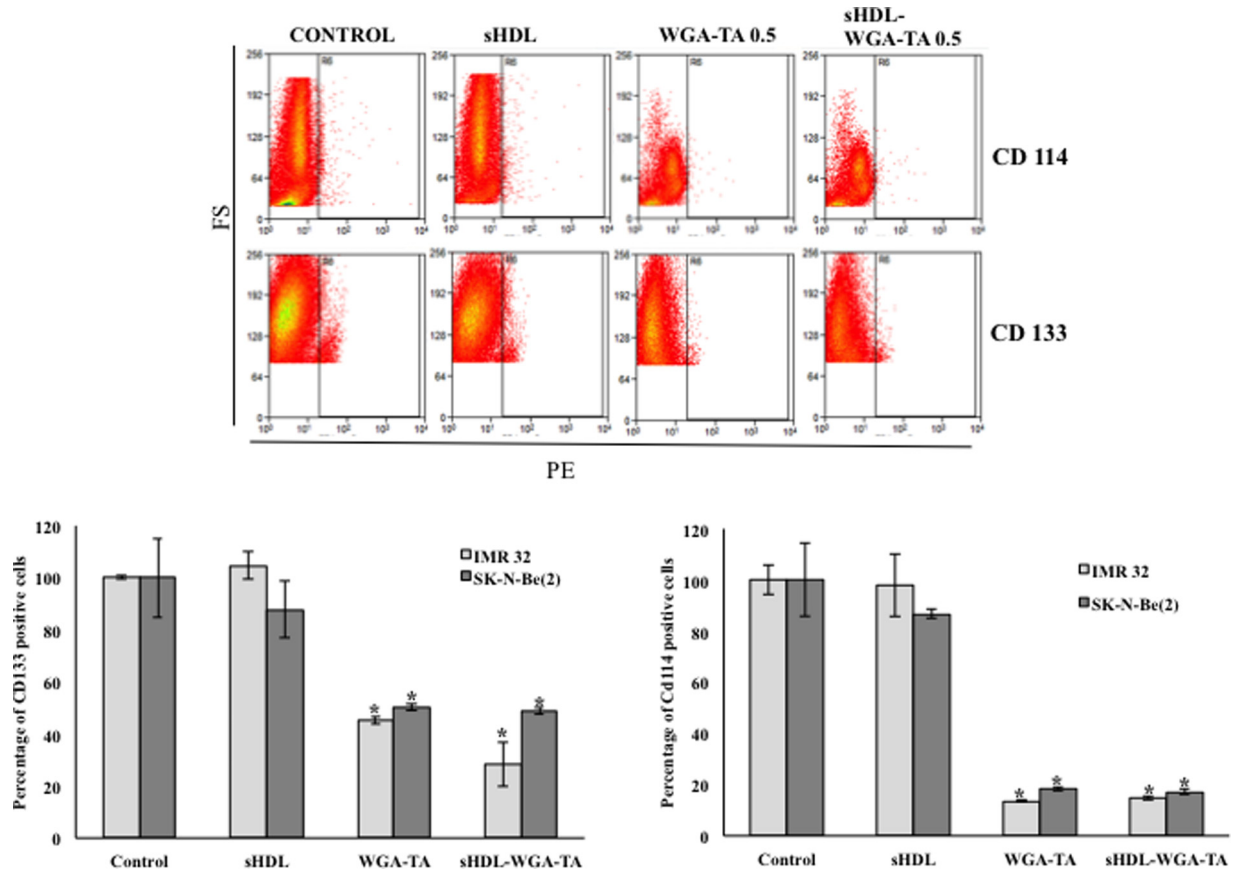

Fig. 5. Markers of NB CSCs are downregulated by WGA-TA–loaded sHDL and WGA-TA. Cell surface markers CD133 and CD114 were analyzed after treatment of human NB cells IMR- 32 and SK-N-BE(2) with drugs (sHDL, WGA-TA, sHDL-WGA-TA). Representative flow cytometry figures are shown for SK-N-BE(2), and the results for both cells are shown below.

Table
IC50 values of NB cells and fibroblast cells after treatment with varying concentrations of drugs (sHDL or WGA-TA or sHDL-WGA-TA).

IC50 in nM	sHDL	WGA-TA	sHDL-WGA-TA
IMR32	9,982 ± 5	24.46 ± 1.43	26.44 ± 0.94
SK-N-BE(2)	>10,000	58.88 ± 3.13	59.26 ± 4.2
SH-EP	>10,000	55.61 ± 1.1	56.21 ± 2.79
SK-N-As	>10,000	21.62 ± 1.1	33.55 ± 3.32
Fibroblast	>10,000	192.5 ± 26.8	283.8 ± 34.9

tumor-bearing mice were performed 24 hours following intraperitoneal injection of either DiR-sHDL or DiR liposomes. The results showed efficient accumulation of the nanoparticles in the tumor (Fig 7, *A*) only in mice injected with sHDL nanoparticle, not in mice injected with liposomes (Supplemental Fig 1). In addition, IVIS imaging also indicated high uptake of the sHDL nanoparticles in the liver, which plays a critical role in regulating cholesterol, whereas other organs showed minimal uptake (Fig 7, *B*).

Discussion

Despite recent advances in chemotherapy and surgery, the long-term survival rate of patients with advanced metastatic NB is a dismal 18% to 30%.[21] Systemic toxicity associated with chemotherapeutic agents is a serious problem, especially in pediatric cancer patients. Hence, novel anticancer compounds from natural products represent a largely untapped resource for development of new treatment options for pediatric tumors such as NB. This area recently has surged given the need for identification of novel compounds with anticancer benefits and low toxicity.[22]

Withanolides are the key bioactive components present in the Solanaceae family of plants, including the Ashwagandha (*Withania somnifera*) plant, whose medicinal properties have been known for decades in Indian Ayurveda medicine. Withanolides are a group of naturally occurring 28-carbon steroidal lactones with an ergostane skeleton in which C-22 and C-26 are oxidized to form a 6-membered δ-lactone ring. Over the last several years, our group has identified and purified more than 40 natural and semisynthetic withanolide compounds with potent antitumor activity from the native *Physalis* plant.[23,24] We have explored the in vitro efficacy and the mechanism of action of novel natural withanolides that have shown potent anticancer properties both in vitro and in vivo in various cancer models with potential for targeting several cancers, including NB.

Previous studies with our lead compound, WGA-TA, exhibited high potency in inducing apoptosis, modulating the cell cycle, and targeting key oncogenic pathway proteins implicated in the poor survival of NB (Oncotarget, 2018). However, the poor water solubility and short half-life of WGA-TA in vivo may limit its use in the clinic. We sought to address these issues by using a nanocarrier that can solubilize the drug and improve the pharmacokinetic profile.

Recently we have reported that sHDLs composed of phospholipids and ApoA-1 mimetic peptides[25] can mimic the function of endogenous HDL to transport cholesterol from peripheral tissues to the liver for metabolism. These sHDL nanoparticles have also been shown to efficiently transport its cargo to SR-B1 expressing tumor cells.[9,26–28] Due to the presence of a hydrophobic space in the lipid

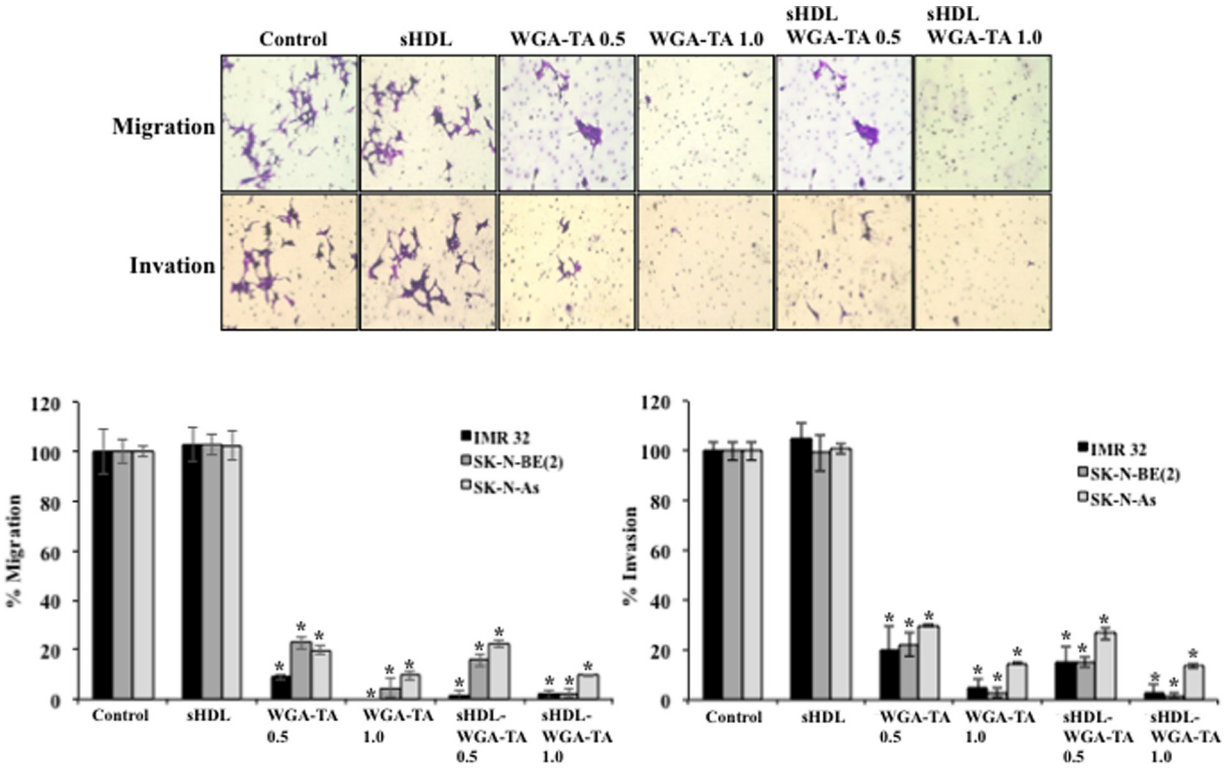

Fig. 6. Dose-dependent blocking of migration and invasion of NB cells by WGA-TA–loaded sHDL and WGA-TA. Boyden chambers coated with Matrigel and controls (uncoated) were used for estimating invasion and migration of NB cells (IMR-32, SK-N-BE(2), and SK-N-AS) after treating them with varying concentrations of either sHDL or WGA-TA or sHDL-WGA-TA nanoparticles for 48 hours. MEM supplemented with 10% FBS was used as a chemoattractant. The number of cells that passed through the membrane was examined by counting the number of cells under a light microscope. Percentage of migration and invasion were calculated after normalization to control untreated cells. Each experiment was repeated thrice, and the values are represented as mean ± standard deviation. Representative figures from IMR-32 cells are shown.

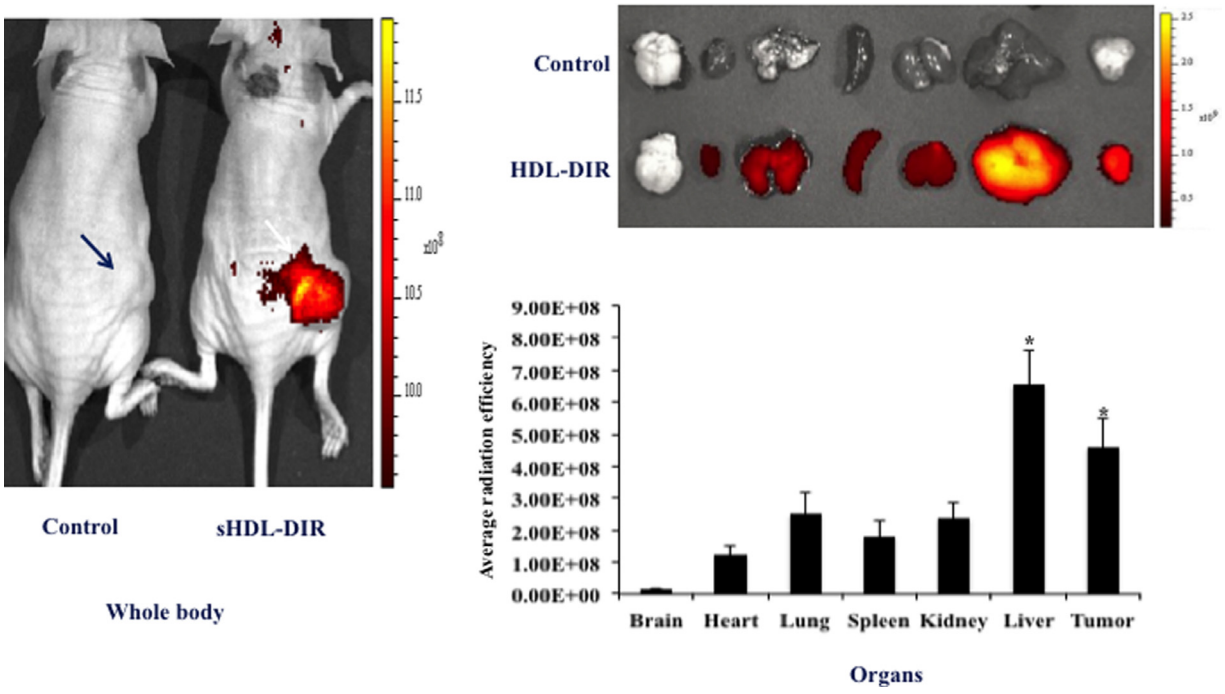

Fig. 7. (*A* and *B*) In vivo uptake of DiR-labeled sHDL nanoparticles by IMR-32 xenografts. (*A*) Approximately 5 million IMR-32 cells were injected into nude mice for developing IMR-32 xenografts. DiR-labeled sHDL nanoparticles were injected intraperitoneally, and images were taken at time 0 and 24 hours post-injection using IVIS imaging system. (*B*) Ex vivo images of organs and tumor at 24 hours. A Representative image from $n = 3$ is shown.

bilayer, sHDL nanoparticles can significantly improve the solubility and transportability of poorly soluble anticancer drugs such as WGA-TA.

Furthermore, sHDLs have been developed and clinically tested for the treatment of atherosclerosis. Clinical trials confirmed that sHDL therapeutics are safe at high doses of 20 to 40 mg/kg infusions and have a prolonged plasma circulation time of 8-14 hours.[29,30] These features of sHDL may overcome the limitations of WGA-TA and facilitate its use in the clinic.

Our results indicate that HDL receptor SR-B1 is highly expressed in NB cells, especially N-myc amplified cells, compared to normal cells. Consistent with previous results with retinoid-encapsulated sHDL that were nontoxic to normal cells, our sHDL-WGA-TA nanoparticles were effective in targeting NB cancer cells without significant effect on normal fibroblast cells.[30] Similar to other malignant cancers,[31] NB cells overexpress SR-B1, and these cells take up the sHDL nanoparticles in an SR-B1-dependent manner. Our novel sHDL delivery system for WGA-TA will be highly suitable for targeting high-risk NBs that are known to have amplified N-myc. NB tumors are heterogeneous, and the CSC model suggests that treatment failure is due to the presence of self-renewal of a small population of tumor-initiating cells.[32] Hence, we examined the self-renewal and migratory properties of NB cells after treatment with sHDL-WGA-TA nanoparticles. Consistent with our previous report in which WGA-TA can target thyroid CSCs prevent self-renewal and migration[33], the sHDL-WGA-TA nanoparticles were able to block both self-renewal and migration in NB-CSCs, whereas sHDL nanoparticles alone had no effect on these CSC functions.

Overall, our results demonstrate that novel withanolide-encapsulated sHDL nanoparticles target NB tumors both in vitro and in vivo through the HDL receptor SR-B1. Additionally, our results suggest that these novel nanoparticles decrease the viability of NB cells and potentially target NB CSC functions such as self-renewal, migration, and invasion. Given these encouraging findings, future in vivo translational studies are warranted to further evaluate this drug's potential as a novel therapy for NB, especially related to its safety and efficacy on CSC inhibition, tumor growth, invasion, and metastatic spread.

Supplementary materials

Supplementary material associated with this article can be found, in the online version, at doi:10.1016/j.surg.2018.01.023.

References

1. Irwin MS, Park JR. Neuroblastoma: paradigm for precision medicine. *Pediatr Clin North Am*. 2015;62(1):225–256.
2. Lau L, Tai D, Weitzman S, Grant R, Baruchel S, Malkin D. Factors influencing survival in children with recurrent neuroblastoma. *J Pediatr Hematol/Oncol*. 2004;26:227–232.
3. Santana VM, Furman WL, McGregor LM, Billups CA. Disease control intervals in high-risk neuroblastoma. *Cancer*. 2008;112:2796–2801.
4. Di Bartolo BA, Nicholls SJ, Bao S, Rye KA, Heather AK, Barter PJ, et al. The apolipoprotein A-I mimetic peptide ETC-642 exhibits anti-inflammatory properties that are comparable to high density lipoproteins. *Atherosclerosis*. 2011;217:395–400.
5. Rink JS, McMahon KM, Zhang X, Chen X, Mirkin CA, Thaxton CS, et al. Knockdown of intraislet IKKβ by spherical nucleic acid conjugates prevents cytokine-induced injury and enhances graft survival. *Transplantation*. 2013;96:877–884.
6. Castel V, Segura V, Berlanga P. Emerging drugs for neuroblastoma. *Expert Opin Emerg Drugs*. 2013;18:155–171.
7. Alhasan AH, Kim DY, Daniel WL, Watson E, Meeks JJ, Thaxton CS, et al. Scanometric microRNA array profiling of prostate cancer markers using spherical nucleic acid-gold nanoparticle conjugates. *Anal Chem*. 2012;84:4153–4160.
8. Grogan PT, Sleder KD, Samadi AK, Zhang H, Timmermann BN, Cohen MS. Cytotoxicity of withaferin A in glioblastomas involves induction of an oxidative stress-mediated heat shock response while altering Akt/mTOR and MAPK signaling pathways. *Invest N Drugs*. 2013;31:545–557.
9. Kuai R, Subramanian C, White P, Timmermann B, Moon J, Cohen M, et al. Synthetic high density lipoprotein nanodiscs for targeted withalongolide delivery to adrenocortical carcinoma. *Int J Nanomedicine*. 2017 press.
10. Samadi AK, Bazzill J, Zhang X, Gallagher R, Zhang H, Gollapudi R, et al. Novel withanolides target medullary thyroid cancer through inhibition of both RET phosphorylation and the mammalian target of rapamycin pathway. *Surgery*. 2012;152:1238–1247.
11. Samadi AK, Tong X, Mukerji R, Zhang H, Timmermann BN, Cohen MS. Withaferin A, a cytotoxic steroid from Vassobia breviflora, induces apoptosis in human head and neck squamous cell carcinoma. *J Nat Prod*. 2010;73:1476–1481.
12. Subramanian C, Zhang H, Gallagher R, Hammer G, Timmermann B, Cohen M. Withanolides are potent novel targeted therapeutic agents against adrenocortical carcinomas. *World J Surg*. 2014;38:1343–1352.
13. White PT, Subramanian C, Motiwala HF, Cohen MS. Natural withanolides in the treatment of chronic diseases. *Adv Exp Med Biol*. 2016;928:329–373.
14. Zhang H, Bazzill J, Gallagher RJ, Subramanian C, Grogan PT, Day VW, et al. Antiproliferative withanolides from Datura wrightii. *J Nat Prod*. 2013;76:445–449.
15. Koduru S, Kumar R, Srinivasan S, Evers MB, Damodaran C. Notch-1 inhibition by Withaferin-A: a therapeutic target against colon carcinogenesis. *Mol Cancer Ther*. 2010;9:202–210.
16. Hahm ER, Moura MB, Kelley EE, Van Houten B, Shiva S, Singh SV. Withaferin A-induced apoptosis in human breast cancer cells is mediated by reactive oxygen species. *PloS One*. 2011;6:e23354.
17. Oh JH, Kwon TK. Withaferin A inhibits tumor necrosis factor-alpha-induced expression of cell adhesion molecules by inactivation of Akt and NF-kappaB in human pulmonary epithelial cells. *Int Immunopharmacol*. 2009;9:614–619.
18. Patil D, Gautam M, Mishra S, Karupothula S, Gairola S, Jadhav S, et al. Determination of withaferin A and withanolide A in mice plasma using high-performance liquid chromatography-tandem mass spectrometry: application to pharmacokinetics after oral administration of Withania somnifera aqueous extract. *J Pharm Biomed Anal*. 2013;80:203–212.
19. Kuai R, Li D, Chen YE, Moon JJ, Schwendeman A. High-density lipoproteins: nature's multifunctional nanoparticles. *ACS Nano*. 2016;10:3015–3041.
20. Subramanian C, Kuai R, Zhu Q, White P, Moon JJ, Schwendeman A, et al. Synthetic high-density lipoprotein nanoparticles: a novel therapeutic strategy for adrenocortical carcinomas. *Surgery*. 2016;159:284–294.
21. Megison ML, Gillory LA, Beierle EA. Cell survival signaling in neuroblastoma. *Anticancer Agents Med Chem*. 2013;13:563–575.
22. Sarkar FH, Li Y. Harnessing the fruits of nature for the development of multi–targeted cancer therapeutics. *Cancer Treatment Rev*. 2009;35:597–607.
23. Zhang H, Samadi AK, Gallagher RJ, Araya JJ, Tong X, Day VW, et al. Cytotoxic withanolide constituents of Physalis longifolia. *J Nat Prod*. 2011;74:2532–2544.
24. Zhang H, Motiwala H, Samadi A, Day V, Aube J, Cohen M, et al. Minor withanolides of Physalis longifolia: structure and cytotoxicity. *Chem Pharm Bull (Tokyo)*. 2012;60:1234–1239.
25. Damiano MG, Mutharasan RK, Tripathy S, McMahon KM, Thaxton CS. Templated high density lipoprotein nanoparticles as potential therapies and for molecular delivery. *Adv Drug Deliv Rev*. 2013;65:649–662.
26. Cruz PM, Mo H, McConathy WJ, Sabnis N, Lacko AG. The role of cholesterol metabolism and cholesterol transport in carcinogenesis: a review of scientific findings, relevant to future cancer therapeutics. *Front Pharmacol*. 2013;4:119.
27. Tang J, Kuai R, Yuan W, Drake L, Moon JJ, Schwendeman A. Effect of size and pegylation of liposomes and peptide-based synthetic lipoproteins on tumor targeting. *Nanomedicine*. 2017;13:1869–1878.
28. Yuan Y, Wen J, Tang J, Kan Q, Ackermann R, Olsen K, et al. Synthetic high–density lipoproteins for delivery of 10-hydroxycamptothecin. *Int J Nanomedicine*. 2016;11:6229–6238.
29. Yang S, Damiano MG, Zhang H, Tripathy S, Luthi AJ, Rink JS, et al. Biomimetic, synthetic HDL nanostructures for lymphoma. *Proc Natl Acad Sci United States Am*. 2013;110:2511–2516.
30. Sabnis N, Pratap S, Akopova I, Bowman PW, Lacko AG. Pre-clinical evaluation of rHDL encapsulated retinoids for the treatment of neuroblastoma. *Front Pediatr*. 2013;1:6.
31. Foit L, Giles FJ, Gordon LI, Thaxton CS. Synthetic high-density lipoprotein-like nanoparticles for cancer therapy. *Expert Rev Anticancer Ther*. 2015;15:27–34.
32. Hsu DM, Agarwal S, Benham A, Coarfa C, Trahan DN, Chen Z, et al. G-CSF receptor positive neuroblastoma subpopulations are enriched in chemotherapy-resistant or relapsed tumors and are highly tumorigenic. *Cancer Res*. 2013;73:4134–4146.
33. White PT, Subramanian C, Zhu Q, Zhang H, Zhao H, Gallagher R, et al. Novel HSP90 inhibitors effectively target functions of thyroid cancer stem cell preventing migration and invasion. *Surgery*. 2016;159:142–151.